nature
structural biology

How vitronectin binds PAI-1 to modulate fibrinolysis and cell migration

Aiwu Zhou[1], James A Huntington[1], Navraj S Pannu[1,2], Robin W Carrell[1] & Randy J Read[1]

The interaction of the plasma protein vitronectin with plasminogen activator inhibitor-1 (PAI-1) is central to human health. Vitronectin binding extends the lifetime of active PAI-1, which controls hemostasis by inhibiting fibrinolysis and has also been implicated in angiogenesis. The PAI-1–vitronectin binding interaction also affects cell adhesion and motility. For these reasons, elevated PAI-1 activities are associated both with coronary thrombosis and with a poor prognosis in many cancers. Here we show the crystal structure at a resolution of 2.3 Å of the complex of the somatomedin B domain of vitronectin with PAI-1. The structure of the complex explains how vitronectin binds to and stabilizes the active conformation of PAI-1. It also explains the tissue effects of PAI-1, as PAI-1 competes for and sterically blocks the interaction of vitronectin with cell surface receptors and integrins. Structural understanding of the essential biological roles of the interaction between PAI-1 and vitronectin opens the prospect of specifically designed blocking agents for the prevention of thrombosis and treatment of cancer.

Plasminogen activator inhibitor-1 (PAI-1) is a plasma protein that has been implicated in the processes of hemostasis, angiogenesis and tumor metastasis. The interaction of PAI-1 with the adhesive glycoprotein vitronectin is at the intersection of these varied processes. Vitronectin activates PAI-1 to inhibit fibrinolysis[1] that, if excessive, can trigger coronary thrombosis[2]. The level of active PAI-1 also directly influences angiogenesis[3,4], and the binding of vitronectin to PAI-1 (ref. 5) affects cell adhesion and motility[6]. As a consequence, elevated PAI-1 activity correlates with poor prognosis in many cancers[3,7].

PAI-1 is an atypical member of the serpin family of serine protease inhibitors; it has an inherently brief half-life[8] because of the spontaneous insertion of its intact reactive center loop into the main β-sheet of the molecule[9], which renders the molecule inactive (**Fig. 1a**). This transition to the inactive latent form is slowed by binding to vitronectin, a glycoprotein of 70 kDa present in both plasma and the extracellular matrix[1,10]. Binding to vitronectin stabilizes active PAI-1 and localizes it to its site of action. Expansion of the main β-sheet of PAI-1, through either the latency transition or cleavage of the reactive center loop, results in disruption of the complex and the release of inactive PAI-1 and unliganded vitronectin. The bulk of experimental evidence suggests that high-affinity binding and stabilization of PAI-1 is mediated by the somatomedin B domain comprising the first 44 residues of vitronectin[5,11,12]. We determined the structure of this domain bound to active PAI-1 to understand how it stabilizes the active state of PAI-1 and why it releases inactive PAI-1.

RESULTS

Crystallization and structure determination

PAI-1 and the somatomedin B domain of vitronectin were both expressed recombinantly for cocrystallization trials. Recombinant PAI-1 was expressed as a constitutively active variant that contains four stabilizing mutations that extend its active half-life from 2 to 145 h (ref. 13). The further stabilizing effect of the binding of somatomedin B to this variant form was shown by an accompanying increase in the melting point of the recombinant PAI-1 from 50 to 70 °C. Somatomedin B bound to PAI-1 in 1:1 stoichiometry to give a tight complex (K_d ~1 nM) that crystallized in two forms. Orthorhombic crystals, with a single complex per asymmetric unit, diffracted to 2.3 Å and provided the solution to the structure (**Fig. 1b**). Hexagonal crystals, with four complexes per asymmetric unit, provided additional confirmation of the location of the binding site on PAI-1 for somatomedin B at a lower (3.2 Å) resolution.

Structure and binding interactions

The structure of somatomedin B (**Fig. 1c**) presents a new protein fold, with the only ordered secondary structure being a single-turn α-helix and a single-turn 3_{10}-helix. The structure reveals the presence of four disulfide bonds (cysteine residues 5–21, 9–39, 19–32 and 25–31), which constrain the polypeptide as a novel disulfide-bonded knot.

In the complex (**Figs. 1b** and **2**), somatomedin B binds across the E and F helices of PAI-1. This general region of PAI-1 was identified as the probable binding site in a review[11] of studies of recombinant mutants, antibody binding and crosslinking experiments. In one of these studies, five single point mutations were found specifically to reduce vitronectin binding: Q55P, F109S, M110T, L116P and Q123K[14]. All but the Q55P mutation are in the immediate vicinity of the binding site (**Fig. 2a**); the Q55P mutation may exert an indirect effect by disrupting helix C (residues 52–62).

The binding interactions in the complex are largely hydrophobic, although there is a strong ionic interaction with Arg101 in the s2A–hE

[1]Department of Haematology, University of Cambridge, Cambridge Institute for Medical Research, Wellcome Trust/MRC Building, Hills Road, Cambridge CB2 2XY, UK. [2]Present address: Leiden Institute of Chemistry, Gorlaeus Laboratories, Leiden University, 2300 RA Leiden, The Netherlands. Correspondence should be addressed to R.J.R. (rjr27@cam.ac.uk).

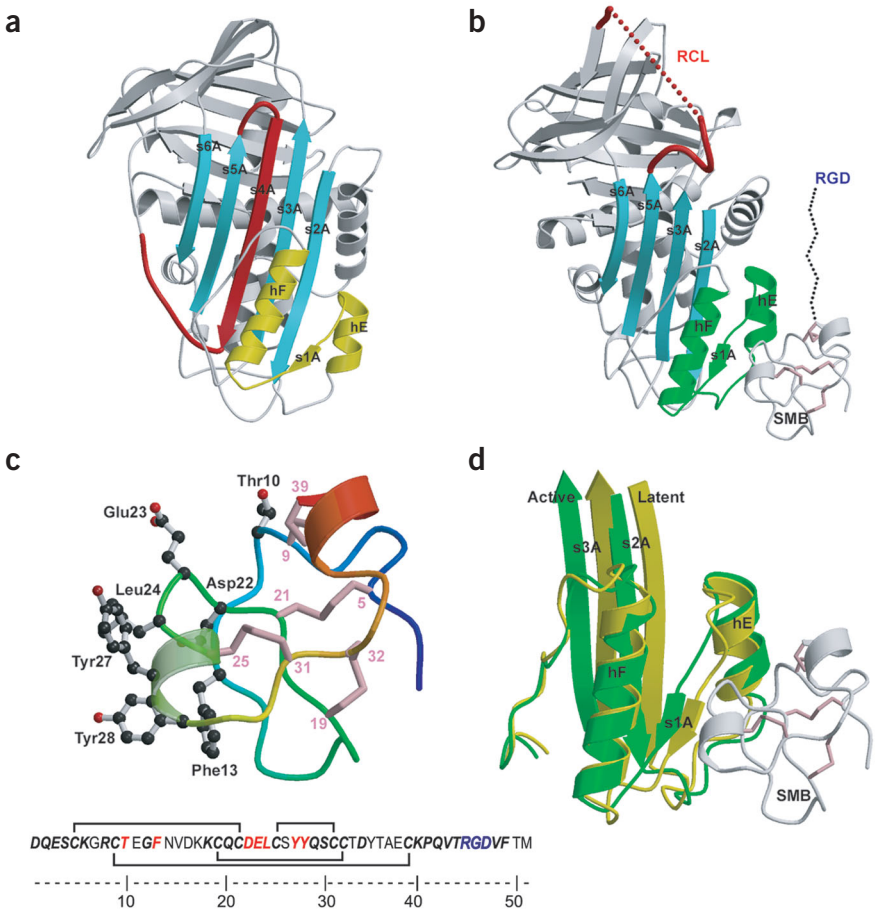

Figure 1 Ribbon diagrams of the complex and its components. (**a**) Latent PAI-1 (ref. 9). In this structure, the reactive center loop is inserted as strand 4 (red) of an expanded sheet A (cyan), changing the shape of the binding site (yellow) for somatomedin B. (**b**) The somatomedin B domain (gray with pink disulfide bridges) binding to the region comprising helix E, strand 1A and helix F (green) of active PAI-1. Dashed lines indicate disordered residues in the reactive center loop (RCL) of PAI-1 and residues leading to the RGD sequence of somatomedin B. (**c**) The somatomedin B domain (blue at N terminus to red at C terminus), showing disulfide bridges (pink) and side chains of residues that interact with PAI-1. The sequence highlights disulfide bridges (brackets), residues conserved among mammalian vitronectin sequences (bold italic), residues with side chains contacting PAI-1 (red) and the RGD motif (blue). (**d**) Comparison of the active (green) and latent (yellow) conformations of PAI-1 showing how the shape of the binding surface changes upon latency.

loop of PAI-1 (**Fig. 2a**). The side chain of Arg101 is almost completely buried in the interface, providing an explanation for the observation that arginine and guanidinium chloride compete in the binding interaction[15]. The shape of the binding surface is substantially different in the inactive six-stranded forms, such as PAI-1 with the reactive center loop cleaved or latent PAI-1 (**Fig. 1d**), consistent with greatly reduced affinity of vitronectin for inactive PAI-1.

DISCUSSION

The structure of the PAI-1–somatomedin B complex suggests a simple mechanism for the stabilization of PAI-1 activity: somatomedin B slows the transition of PAI-1 to the latent form by blocking the associated sliding movement of strands 1 and 2 of the main β-sheet into the gap between helices E and F (**Fig. 1d**). A similar mechanism, in which expansion of the main β-sheet is inhibited, had been suggested on the basis of the location of residues of PAI-1 implicated in the binding interaction[10,14].

The binding to PAI-1 of the somatomedin B domain of vitronectin also exerts more profound effects by directly blocking the interaction of vitronectin with the cell-surface integrins required for cellular motility[6] and with the receptor for cell-bound urokinase-type plasminogen activator (uPAR)[16]. The somatomedin B domain of vitronectin contains a specific binding site for the receptor for uPAR, which has been suggested to overlap with the binding site for PAI-1 (ref. 16). Residues implicated in uPAR binding are clearly blocked in the complex with PAI-1 (**Fig. 2a**). PAI-1 can also regulate cell migration in the extracellular matrix by blocking the interaction between integrin αVβ3 and the RGD integrin-binding site in vitronectin. In a complex with PAI-1, the RGD sequence (residues 45–47 of the somatomedin B domain, **Fig. 1b,c**) will be positioned close to PAI-1, together with the rest of the large vitronectin molecule, leaving insufficient room for the RGD sequence to bind to integrins in the manner seen in the recent crystal structure of the integrin–RGD ligand complex[17]. PAI-1 serves as a switch controlling the interactions of vitronectin; its affinity for vitronectin drops 100-fold when it reacts with target proteinases such as uPA[10], with its release exposing binding sites on vitronectin for uPAR (to which uPA is typically bound) and integrins.

Thus, the preferential binding of the somatomedin B domain by PAI-1 leads to a concordance of events—activation of PAI-1 and the steric blocking of cell surface interactions with vitronectin. The levels of active PAI-1 control angiogenesis[3,4] and the blocking of binding sites on vitronectin directly affects cell migration[6]. Imbalances in these processes have particular significance in malignancy, and there is now convincing evidence that elevated levels of active PAI-1 directly favor the growth and dissemination of tumors. In mice with deficient expression of PAI-1, tumor invasion and vascularization by malignant keratinocytes was prevented but was subsequently restored by transgenic expression of PAI-1 (ref. 18). Clinical studies of thousands of cases of breast cancer[7], together with smaller but consistent studies of a range of other tumors[19], all show a correlation between increased PAI-1 levels and decreased lengths of remission or overall survival.

Paradoxically, elevated levels of uPA, one of the target proteinases of PAI-1, are also associated with a poor prognosis in cancer[7]. This implies that PAI-1 and uPA do not simply act as antagonists. One hypothesis is that a balanced level of PAI-1 and uPA is required to alternately disrupt and re-form interactions of vitronectin with uPAR

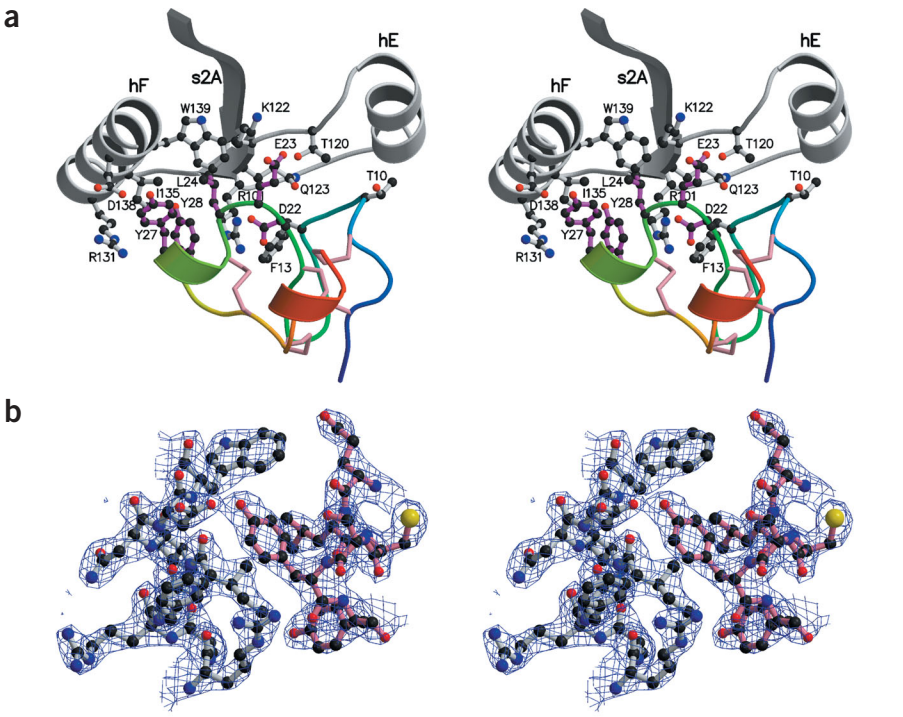

Figure 2 Stereo view of interacting residues in the PAI-1–SMB interface. (**a**) The region of the somatomedin B domain that interacts with PAI-1 overlaps extensively with that involved in the interaction with uPAR, as alanine-scanning mutagenesis has shown that residues Asp22, Glu23, Leu24, Tyr27 and Tyr28 of vitronectin (highlighted with magenta bonds) are important for the interaction with uPAR[16]. Somatomedin B coloring ranges from blue at the N terminus to red at the C terminus. (**b**) Electron density from the final σ_A-weighted[26] map showing the interaction between helix F (hF) of PAI-1 (gray bonds) and the loop comprising residues 23–28 of SMB (pink bonds). The map is contoured at a level of 1.25× the r.m.s. electron density. For clarity, contours >2 Å from an atom in the figure are omitted.

at the leading edge of cell migration[3]. A second hypothesis is that the reaction of PAI-1 with uPA in its complex with uPAR causes the assembly to be endocytosed by the low-density lipoprotein receptor–related protein (LRP), thus breaking interactions mediated by uPAR[20]. These hypotheses are not mutually exclusive and may apply to different cell types with different balances of adhesive factors.

Not surprisingly, there has been much interest in the development of agents to block binding of PAI-1 to vitronectin. Natural products including fungal agents and a wide range of small drugs have been tested[21] but the search has been hindered by the lack of a definitive binding site. Here we see that high-affinity binding takes place at a site that is both circumscribed and precise, and therefore an appropriate target for the specific design of blocking agents. Such agents would not only be prospects for use in treating cancer but would have potential applications as antithrombotic agents.

Table 1 Data and refinement statistics

Diffraction data	
Resolution (Å)[a]	45.0–2.28 (2.37–2.28)
Unique reflections[a]	20,251 (2,204)
Redundancy[a]	12.2 (7.0)
Completeness (%)[a]	99.95 (99.95)
R_{merge}[a,b]	0.112 (0.733)
Refinement	
R_{cryst}[a]	0.196 (0.272)
R_{free}[a]	0.252 (0.343)
Number of atoms	
Protein	3,187
Solvent	137
R.m.s. deviation from ideality	
Bonds (Å)	0.012
Angles (°)	1.3
Average *B*-value (Å^2)	
PAI-1[c]	26.0 (42.1)
Somatomedin B[c]	31.8 (67.5)
Solvent	44.1

[a]Numbers in parentheses refer to high-resolution shell. [b]$R_{merge} = \Sigma|I - \langle I\rangle| / \Sigma I$. [c]Values in parentheses include isotropic equivalent of TLS contribution.

METHODS

Protein preparation. The recombinant PAI-1 stable quadruple mutant[13] was prepared as described. To prepare the recombinant somatomedin B domain, the DNA fragment encoding the first 110 amino acids of vitronectin[22], together with a His_6-tag and a Met at the N terminus, was cloned into expression vector pGEX-4T2 (Amersham). The recombinant somatomedin B domain was expressed as a fusion protein with glutathione *S*-transferase in *E. coli* strain AD494(DE3) (Novagen), purified by nickel-chelating column following the standard procedure and lyophilized after dialysis against water. Both the recombinant fusion protein and plasma vitronectin were digested with a 100-fold molar excess of CNBr in 10 mM HCl at room temperature for 16 h, and the digest was analyzed on a Prodigy ODS3 column (Phenomenex) with a 10–40% (v/v) methyl cyanide (MeCN) gradient in 0.1% (v/v) trifluoroacetic acid (TFA). The 51-amino-acid peptide containing the somatomedin B domain and RGD motif of vitronectin, denoted as the SMB peptide, was identified by liquid chromatography–mass spectrometry and N-terminal protein sequencing. This recombinant SMB has an HPLC retention time identical to that of SMB derived from human plasma vitronectin. The fractions containing SMB were collected, further purified on the Prodigy ODS3 column and lyophilized. The molecular weight of SMB (both recombinant and plasma-derived forms) was determined by electron spray mass spectrometry to be 5,762 Da (the C-terminal methionine is converted to lactone). The difference of 8 Da from the calculated molecular weight of 5,770 Da indicates that the eight cysteine residues form four disulfide bonds. Fluorescence titration showed that SMB binds to PAI-1 at a 1:1 molar ratio, and a thermal stability study by CD showed that the PAI-1–SMB complex has a melting point of 70 °C, 20 °C higher than that of PAI-1.

Crystallization, data collection and structure solution. The PAI-1 mutant (3 mg ml^{-1}) was mixed with SMB at a 1:1 molar ratio in 10 mM sodium acetate and 50 mM NaCl. Crystals of the complex were grown at 4 °C by the hanging-

drop method, mixing 1 μl of complex solution with 1 μl of well solution (2–9% (w/v) PEG 12000 and 50 mM HEPES, pH 7.4). Crystals grew to full size in 2 weeks. These crystals were hexagonal (space group $P6_1$, with $a = b = 92.7$ Å and $c = 504.7$ Å), with four complexes per asymmetric unit, and generally suffered from twinning. Data were collected to a resolution of 3.2 Å at beamline 14.2 of the Daresbury SRS. Four copies of the active PAI-1 structure[23] were positioned in the asymmetric unit by molecular replacement. The resulting map showed electron density between helices E and F of all four copies of PAI-1 but could not be interpreted in detail at this resolution. The addition of 0.5 μl of 50% (v/v) PEG 400 to the drops yielded a new orthorhombic crystal form in space group $P2_12_12_1$ with $a = 47.50$ Å, $b = 90.09$ Å and $c = 100.16$ Å. Data for the orthorhombic form were collected to a resolution of 2.3 Å from a single frozen crystal on APS beamline 19-ID and processed with HKL2000 (ref. 24). The structure was solved by molecular replacement with Beast[25], using the structure of the stable mutant of PAI-1 in the active conformation[23] as a model. The SMB domain was built into σ_A-weighted[26] electron density phased with the incomplete model using O[27] and refined using a translation, libration, screw (TLS) model of thermal motion in REFMAC5 (ref. 28). Other calculations were carried out with programs from the CCP4 suite[29]. The final model includes residues 6–337 and 348–379 of PAI-1 and 3–39 of SMB. Crystallographic statistics are presented in **Table 1**. The structure was validated with PROCHECK[30]; 89.9% of residues are in the most favored regions of the Ramachandran plot, with only one residue in the generously allowed region and none in the dis-allowed region. Molecular graphics figures were prepared with MolScript[31] and Raster3D[32], with the exception of electron density in **Figure 2b**, which was prepared with BobScript[33] and Raster3D[32].

Coordinates. Atomic coordinates and structure factors have been deposited in the Protein Data Bank (accession code 1OC0).

ACKNOWLEDGMENTS

We thank N. Duke for assistance in collecting data at the APS and A. McCoy for advice on fitting the somatomedin B domain to the initial electron density maps. H. Ogawa kindly provided cDNA for vitronectin. Use of the SBC beamline at the APS was supported by the US Department of Energy Office of Biological and Environmental Research. Beamtime at station 14.2 of Daresbury SRS was provided by CLRC Daresbury Laboratory. R.J.R. and R.W.C. were supported by the Wellcome Trust (UK) and J.A.H. by the Medical Research Council (UK) and National Institutes of Health (USA).

COMPETING INTERESTS STATEMENT

The authors declare that they have no competing financial interests.

Received 28 February; accepted 22 May 2003
Published online 15 June 2003; doi:10.1038/nsb943

1. Preissner, K.T. *et al.* Structural requirements for the extracellular interaction of plasminogen activator inhibitor-1 with endothelial cell matrix-associated vitronectin. *J. Biol. Chem.* **265**, 18490–18498 (1990).
2. Kohler, H.P. & Grant, P.J. Plasminogen activator inhibitor type 1 and coronary heart disease. *N. Engl. J. Med.* **342**, 1792–1801 (2000).
3. McMahon, G.A. *et al.* Plasminogen activator inhibitor-1 regulates tumor growth and angiogenesis. *J. Biol. Chem.* **276**, 33964–33968 (2001).
4. Devy, L. *et al.* The pro- or antiangiogenic effect of plasminogen activator inhibitor 1 is dose dependent. *FASEB J.* **16**, 147–154 (2002).
5. Seiffert, D. & Loskutoff D.J. Evidence that type 1 plasminogen activator inhibitor binds to the somatomedin domain of vitronectin. *J. Biol. Chem.* **266**, 2824–2830 (1991).
6. Stefansson, S. & Lawrence, D.A. The serpin PAI-1 inhibits cell migration by blocking integrin $\alpha_V\beta_3$ binding to vitronectin. *Nature* **383**, 441–443 (1996).
7. Look, M.P. *et al.* Pooled analysis of prognostic impact of urokinase-type plasminogen activator and its inhibitor PAI-1 in 8377 breast cancer patients. *J. Natl. Cancer Inst.* **94**, 116–128 (2002).
8. Hekman, C.M. & Loskutoff, D.J. Endothelial cells produce a latent inhibitor of plasminogen activators that can be activated by denaturants. *J. Biol. Chem.* **260**, 11581–11587 (1985).
9. Mottonen, J. *et al.* Structural basis of latency in plasminogen-activator inhibitor-1. *Nature* **355**, 270–273 (1992).
10. Lawrence, D.A. *et al.* Characterization of the binding of different conformational forms of plasminogen activator inhibitor-1 to vitronectin. *J. Biol. Chem.* **272**, 7676–7680 (1997).
11. Schroeck, F., Arroyo de Prada, N., Sperl, S., Schmitt, M. & Magdolen, V. Interaction of plasminogen activator inhibitor type-1 (PAI-1) with vitronectin (Vn): mapping the binding sites on PAI-1 and Vn. *Biol. Chem.* **383**, 1143–1149 (2002).
12. Okumura, Y. *et al.* Kinetic analysis of the interaction between vitronectin and the urokinase receptor. *J. Biol. Chem.* **277**, 9395–9404 (2002).
13. Berkenpas, M.B., Lawrence, D.A. & Ginsburg, D. Molecular evolution of plasminogen activator inhibitor-1 functional stability. *EMBO J.* **14**, 2969–2977 (1995).
14. Lawrence, D.A., Berkenpas, M.B., Palaniappan, S., & Ginsburg, D. Localization of vitronectin binding domain in plasminogen activator inhibitor-1. *J. Biol. Chem.* **269**, 15223–15228 (1994).
15. Sigurdardottir, O. & Wiman, B. Studies on the interaction between plasminogen activator inhibitor-1 and vitronectin. *Fibrinolysis* **6**, 27–32 (1992).
16. Deng, G., Curriden, S.A., Wang, S., Rosenberg, S. & Loskutoff, D.J. Is plasminogen activator inhibitor-1 the molecular switch that governs urokinase receptor-mediated cell adhesion and release? *J. Cell Biol.***134**, 1563–1571 (1996).
17. Xiong, J.-P. *et al.* Crystal structure of the extracellular segment of integrin αVβ3 in complex with an Arg-Gly-Asp ligand. *Science* **296**, 151–155 (2002).
18. Bajou, K. *et al.* Absence of host plasminogen activator inhibitor 1 prevents cancer invasion and vascularization. *Nat. Med.* **4**, 923–928 (1998).
19. Harbeck, N. *et al.* Clinical relevance of the plasminogen activator inhibitor type 1 — a multifaceted proteolytic factor. *Onkologie* **24**, 238–244 (2001).
20. Czekay, R.-P., Aertgeerts, K., Curriden, S.A. & Loskutoff, D.J. Plasminogen activator inhibitor-1 detaches cells from extracellular matrices by inactivating integrins. *J. Cell Biol.* **160**, 781–791 (2003).
21. Gils, A. *et al.* Characterization and comparative evaluation of a novel PAI-1 inhibitor. *Thromb. Haemost.* **88**, 137–143 (2002).
22. Yoneda, A., Ogawa, H., Kojima, K. & Matsumoto, I. Characterization of the ligand binding activities of vitronectin: interaction of vitronectin with lipids and identification of the binding domains for various ligands using recombinant domains. *Biochemistry* **37**, 6351–6360 (1998).
23. Sharp, A.M. *et al.* The active conformation of plasminogen activator inhibitor 1, a target for drugs to control fibrinolysis and cell adhesion. *Structure Fold. Des.* **7**, 111–118 (1999).
24. Otwinowski, Z. & Minor, W. Processing of X-ray diffraction data collected in oscillation mode. *Methods Enzymol.* **276**, 307–326 (1997).
25. Read, R.J. Pushing the boundaries of molecular replacement with maximum likelihood. *Acta Crystallogr. D* **57**, 1373–1382 (2001).
26. Read, R.J. Improved Fourier coefficients for maps using phases from partial structures with errors. *Acta Crystallogr. A* **42**, 140–149 (1986).
27. Jones, T.A., Zou, J.Y., Cowan, S.W. & Kjeldgaard, M. Improved methods for building protein models in electron density maps and the location of errors in these models. *Acta Crystallogr. A* **47**, 110–119 (1991).
28. Winn, M.D., Isupov, M.N. & Murshudov, G.N. Use of TLS parameters to model anisotropic displacements in macromolecular refinement. *Acta Crystallogr. D* **57**, 122–133 (2001).
29. Collaborative Computational Project, Number 4. The CCP4 suite: programs for protein crystallography. *Acta Crystallogr. D* **50**, 760–763 (1994).
30. Laskowski, R.A., Moss, D.S. & Thornton, J.M. Main-chain bond lengths and bond angles in protein structures. *J. Mol. Biol.* **231**, 1049–1067 (1993).
31. Kraulis, P.J. MOLSCRIPT: a program to produce both detailed and schematic plots of protein structures. *J. Appl. Crystallogr.* **24**, 946–950 (1991).
32. Merritt, E.A. & Bacon, D.J. Raster3D photorealistic molecular graphics. *Methods Enzymol.* **277**, 505–524 (1997).
33. Esnouf, R.M. An extensively modified version of MolScript that includes greatly enhanced coloring capabilities. *J. Mol. Graph. Model.* **15**, 132–134 (1997).